30. Halmschlager, E., Butin, H. and Donaubauer, E., *Eur. J. For. Pathol.*, 1993, **23**, 51–63.
31. Rodrigues, K. F., *Mycologia*, 1994, **86**, 376–385.
32. Shankar Raman, T. R., Menon, R. K. G. and Sukumar, R., *J. Bombay Nat. Hist. Soc.*, 1996, **93**, 178–192.
33. Petrini, O., in *Microbial Ecology of Leaves* (eds Andrews, J. A. and Hirano, S. S.), Springer-Verlag, New York, 1991, pp. 179–197.
34. Petrini, O., in *Microbiology of the Phyllosphere* (eds Fokkema, N. J. and van den Huevel, J.), Cambridge University Press, Cambridge, 1986, pp.175–187.
35. Suresh, G., Narasimhan, N. S., Masilamani, S., Partho, P. D. and Geetha, G., *Phytoparasitica*, 1997, **25**, 33–39.
36. Okane, I., Nakagiri, A. and Ito, T., *Can. J. Bot.*, 1998, **76**, 657–663.

ACKNOWLEDGEMENT. We thank Dr John A. Johnson, University of New Brunswick, Canada, for critically reading the manuscript and for his suggestions.

Received 27 January 2000; revised accepted 13 March 2000

Analysis of a north-south magnetic profile over the Central Indian Ocean

S. Rajendran[†,*] and T. K. S. Prakasa Rao[‡]

[†]Department of Marine Geology and Geophysics, Cochin University of Science and Technology, Cochin 682 016, India
[‡]Department of Geophysics, Andhra University, Visakhapatnam 530 003, India

Marine magnetic anomalies provide valuable information on the nature and evolution of the oceanic crust. Magnetic profiles aligned along the direction of spreading enable us to calculate the spreading rates of oceanic crusts on which they pass. This can be done with computed profiles assuming the model and magnetic reversal time scale of the earth. In the present study the north-south magnetic profile of 1280 nautical miles extending from 15°30′S, 77°E to 6°N, 79°E in the Central Indian Ocean is analysed. The profile runs between the 76°30′E and 79°E Fracture Zones passing over part of the Australian plate, the Central Indian Ocean deformation zone and part of the Indian plate along the Comorin Ridge. The analysis shows that the profile has a continuous sequence of prominent age anomalies from 22 to 34 N. Australian plate and deformation zone segments have well preserved continuous age anomalies from 22 to 33 and thus their spreading rates are calculated. The results show that the profile is characterized by sets of anomalies with varied spreading rates, anomalies 23–30 having higher values compared to the rest. The spreading rate of anomalies 22–27 is 7.8 cm/yr whereas for anomalies 27–30 it is 10.3 cm/yr. Anomalies 30–33 have a moderate spreading rate of 4.6 cm/yr. Another interesting feature is that the profile has the characteristic edge-effect anomaly on the segment over the Indian plate indicating the oceanic–continental crust boundary.

*For correspondence

McKENZIE and Sclater[1], Sclater and Fisher[2] and Schlich[3] have studied broad regional tectonic features of the Indian Ocean. Detailed investigations by Royer and Schlich[4], Patriat and Segoulin[5], Royer *et al.*[6] and Munschy and Schlich[7] have contributed to the understanding of the evolution of the Indian Ocean. Magnetic anomalies of the Indian Ocean are well preserved due to the absence of active trenches except the Indonesian trench in eastern Indian Ocean. Earlier studies revealed that the major basins lying between spreading ridges, continental margins and submarine ridges evolved during three main phases since the break-up of the Gondwana in the Late Jurassic, the three phases being Late Jurassic to mid-Cretaceous, mid-Cretaceous to Middle Eocene and Middle Eocene to Present. The Central Indian Basin between Central Indian Ridge and Ninetyeast Ridge, bounded in the south by the south-east Indian Ridge and the Indian Ocean Triple Junction, has a complex evolutionary history. The complexity is caused mainly by the variations in spreading rates. Between anomalies 32 and 21, i.e. between 80 and 50 Ma, rapid spreading took place about two east-west ridges separated by a long north-south fracture zone (Chagos–Laccadive lineament) which was uninterrupted during this epoch[1]. The intense tectonic deformation of sediments and the basement in the equatorial region of the Central Indian Basin displays clear evidence of intraplate lithospheric deformation on long wavelength (100–300 km) and short wavelength (5–20 km) scales. The nature of deformation can be visualized from seismicity[8,9], geoid and gravity anomalies[10] and anomalous heat flow[11]. Seismic reflection studies in the Central Indian Ocean[12–17] revealed undulations of the basement in an E-W lineated pattern. The basement highs and lows have correlation with the geoid anomalies[18]. The characteristic edge-effect anomaly in the Comorin Ridge of the Indian plate was reported by Kahle *et al.*[19]. They delineated the oceanic–continental crust boundary by isostatic and free air anomaly studies. The present magnetic study, apart from providing spreading rates of a continuous sequence of age anomalies of the profile, supplements information on the oceanic–continental crust boundary with the edge-effect anomaly.

Figure 1 shows the M9M9 magnetic profile which extends from 15°30′S, 77°E to 6°N, 79°E covering a total distance of 1280 nautical miles in the Central Indian Ocean. The profile is aligned almost in the direction of spreading which took place during the second phase (mid-Cretaceous to the Middle Eocene) of the Indian Ocean evolution. The limits of the deformed zone within the study area are adopted from Gordon and DeMets[20]. In a recent work in this area, a new fracture zone was recognized at 76°30′E

with an orientation of N12°E (ref. 21) which was subsequently interpreted as trace of the Indian Ocean Triple Junction. Although its length has not been assessed, it is found parallel to 79°E and 83°E Fracture Zones. The M9M9 profile is located in the compartment between 76°30′E Fracture Zone and the 79°E Fracture Zone (Indrani FZ) and is uninterrupted by any major topographic features. The submarine topography of the study area is comparatively smooth except for some E-W trending small ridges. This area also covers the region south of the NE-SW diffuse zone of high seismicity with a predominantly N-S compression as proposed by Neprochnov *et al.*[22] and Levchenko *et al.*[23].

The magnetic data were collected during 1984 as part of a project, carried out by the National Institute of Oceanography, Goa, India using the EG&G GeoMetrics Marine magnetometer. The bathymetric data were collected with a 12 kHz Deep-Sea Raytheon Echosounder. For position fixing SatNav system (Magnovox) was used. The total magnetic intensity data collected in the analogue form were digitized at an interval of 1 nautical mile and reduced by subtracting the value of the IGRF (1985) at each point. From the reversal chronology[24] and a uniform spreading rate, a magnetic model of the ocean floor is built consisting of normally and reversely magnetized rectangular strips of infinite length in a direction at right angles to the direction of spreading. The magnetic anomaly computed from the model is made to fit the observed profile by adjusting the spreading rate. Assuming the ridge axis to be near 40°S and spreading direction as N10°E the synthetic curve for the M9M9 profile was generated as shown in Figure 3.

The magnetic sequence (anomalies 22–33) corresponding to the Paleocene and Late Cretaceous was properly identified using a set of N-S magnetic profiles, M1M1 and M2M2 extending from 18°S to 4°N along longitudes 80°E and 81°E respectively[25] (Figure 1). As seen from Figure 2, the anomalies 22–27 are well preserved and distinct over the Australian plate except the contamination in anomaly 23. The contamination could be due to the east-west trending linear feature having a relief of 200 to 500 m. Anomalies 28–33 are clearly identified in spite of the tectonic manifestation in the Central Indian Ocean deformed zone which extends from 8°S to the equator. However, these anomalies have lesser clarity than anomalies 22–27 observed in the Australian plate segment. The spreading rates shown in Tables 1 and 2 correspond to the Australian plate and the deformed zone, respectively. The spreading rates are comparable to those calculated by earlier workers except the slow spreading of anomaly 32 being 2.6 cm/yr. This slow spreading is observed in other parallel profiles along 81°E and 82°E as well[25]. Present calculations show that the average spreading rate in the Australian plate area (anomaly 22–27) is 7.8 cm/yr and in the Central Indian deformed zone (anomaly 28–33) it is 5.4 cm/yr. McKenzie and Sclater[1] obtained for the Central Indian Basin a spreading rate of about 8.0 cm/yr for anomalies 23–30 and 5.6 cm/yr for anomalies 30–33. Sclater and Fisher[2] calculated the average spreading rates

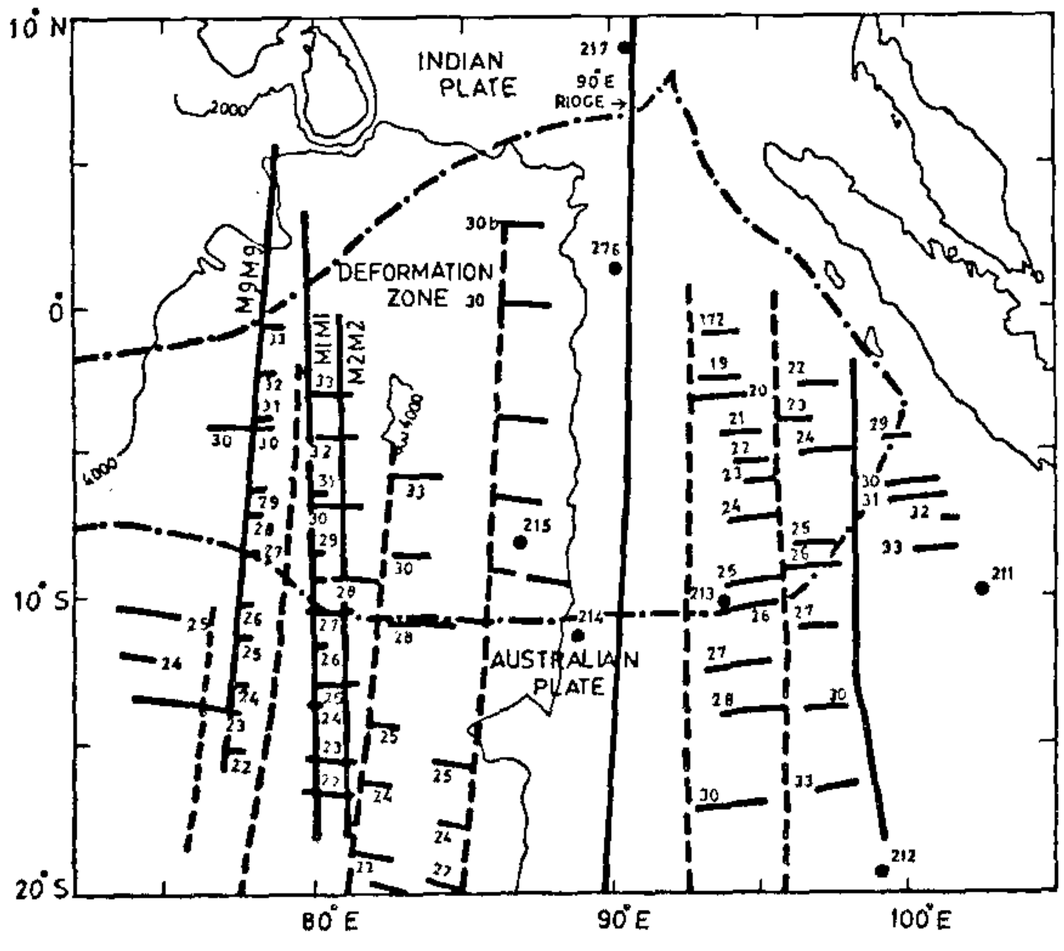

Figure 1. Alignment of M9M9 magnetic profile in the Central Indian Ocean (base map adapted from Sclater and Fisher[2]). Deformation zone (adapted from Gordon and DeMets[20]) is shown within dotted lines. Heavy numbered lines along M9M9, M1M1 and M2M2 represent magnetic anomalies identified by the authors. North-south dashed lines represent the fracture zones. North-south continuous heavy line along 90°E longitude represents the 90°E Ridge.

Table 1. Spreading rates within the Australian plate

Anomaly No.	Spreading rate (cm/yr)	Average value (cm/yr)
22	4.1	
23	9.1	
24	7.9	7.8
25	7.8	
26	8.8	
27	10.5	

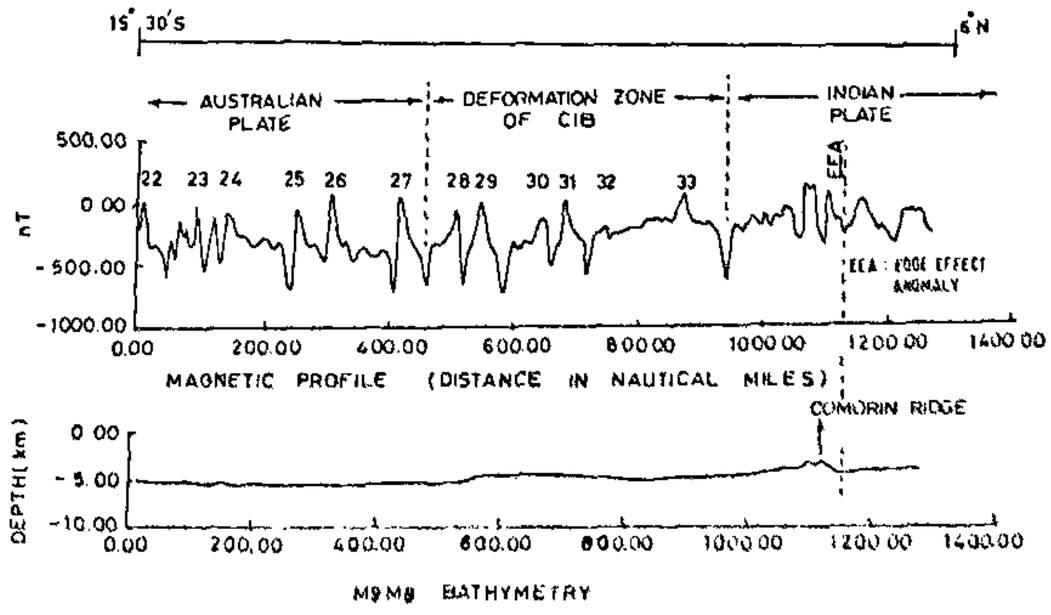

Figure 2. Magnetic profile M9M9 traversing Australian plate, deformation zone and the Indian plate with age anomalies (top) and bathymetry (bottom).

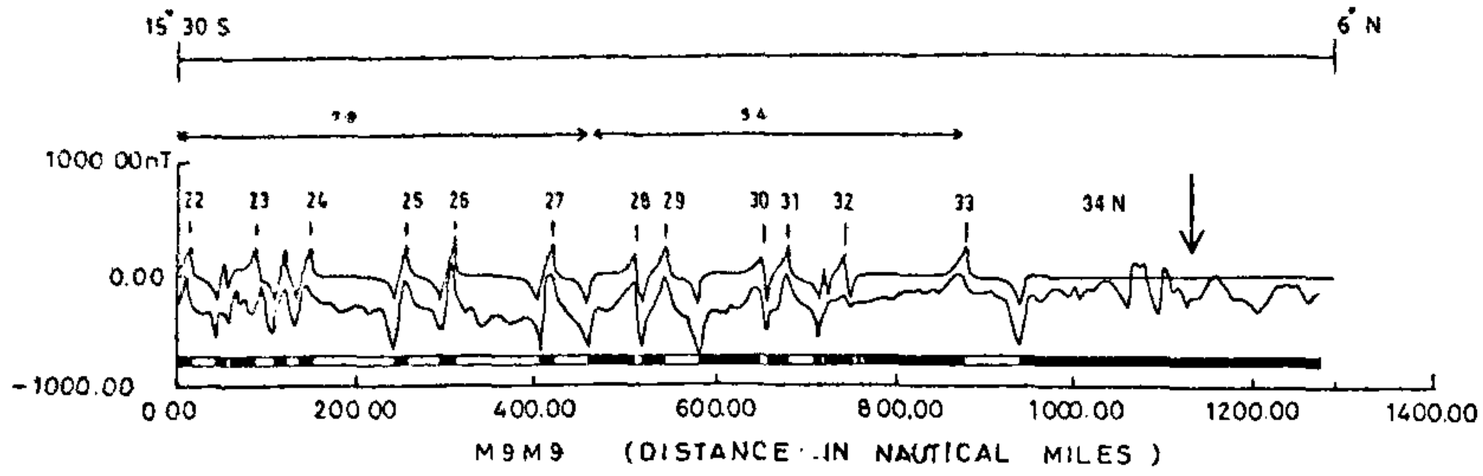

Figure 3. Magnetic profile M9M9 with age anomalies marked along with the synthetic anomaly profile and block model. 34 N extends up to vertical arrow which shows the oceanic–continental crust boundary.

Table 2. Spreading rates within the deformed zone

Anomaly No.	Spreading rate (cm/yr)	Average value (cm/yr)
28	11.2	
29	9.8	
30	10.0	5.4
31	4.7	
32	2.6	
33	4.3	

Table 3. Comparison of spreading rates

Phases	Sclater and Fisher[2] (cm/yr)	Present study (cm/yr)
Anomaly 17–22	4.0	–
Anomaly 22–27	8.1	7.8
Anomaly 27–30	12.0	10.3
Anomaly 30–33	5.7	4.6

for anomalies 22–27, 27–30 and 30–33 as 8.1 cm/yr, 12 cm/yr and 5.7 cm/yr respectively, whereas corresponding spreading rates (Table 3) from the present study are 7.8 cm/yr, 10.3 cm/yr and 4.6 cm/yr. The high spreading rate of the Indian Ocean lithosphere during 63 to 68 Ma (corresponding to anomaly 28–30) has been interpreted by Raval[26] as matching the maximal energy phase of the plume associated with Deccan volcanism. North of the equator the profile has neither reversals nor anomalies related to Mesozoic age, indicating that the above part is clearly a succession of anomaly 33, i.e. 34 N (Cenozoic Magnetic Quiet Zone; Figure 3). Although anomaly 34 N is identified on the Indian plate, the type of signatures does not permit calculation of the rate of spreading.

The Comorin Ridge trends NNW-SSE linearly from 2° to 6°N and from 77° to 79°E. The bathymetric profile shows a conspicuous positive feature in the northern portion between 2°N and 5°N (1125 miles, Figure 2). The first half of the above profile is very smooth from the south and the latter half rises gently with a small gradient. The ridge has an elevation of about 1000 m. Studies on passive continental margins such as those of South Africa, Falkland Plateau, South Brazil and Australia have revealed the presence of conspicuous linear magnetic and gravity anomalies[27,28]. These anomalies are commonly referred to as structural boundaries in the earth's crust. In many cases, topographic and basement highs or ridges are present along these boundaries[29–32]. The ridge type features are characterized by pronounced positive isostatic gravity anomalies and high-amplitude, short-wavelength magnetic anomalies. The isostatic highs followed by lows with a steep gradient mark the boundary between oceanic and rifted or altered continental crust[19,27]. Kahle *et al.*[19] observed positive isostatic anomalies over the Comorin Ridge, a steep isostatic gradient along its entire landward edge and a pronounced decrease in isostatic anomalies east of Comorin Ridge. They suggested that the boundary deciphered is the boundary between oceanic and rifted or altered continental crust. In the present study the northern segment of the profile (Figures 2 and 3) over the Indian plate shows the oceanic and continental crust boundary by the characteristic edge-effect anomaly. In Figure 2, at 1125 miles, the edge-effect anomaly is clearly evidenced by the transition from oceanic to continental signature further confirming the conclusions derived by Kahle *et al.*[19].

The profile M9M9, ideally aligned in the spreading direction of the second phase (mid-Cretaceous–the Middle Eocene) of the Indian Ocean evolution history, presents a continuous sequence of age anomalies from 22 to 34 N. Age anomalies have been recognized over the Central Indian Ocean deformation zone in spite of the tectonic disturbances in this area. The spreading rates calculated from M9M9 for the three consecutive phases of the second period (anomalies 17–33) are 7.8 cm/yr for anomalies 22–27, 10.3 cm/yr for anomalies 27–30 and 4.6 cm/yr for anomalies 30 –33. The average spreading rate in the Australian plate area is 7.8 cm/yr and in the deformed zone is 5.4 cm/yr. The Indian plate segment of the magnetic profile demarcates the oceanic–continental crust boundary with the characteristic edge-effect anomaly.

1. McKenzie, D. P. and Sclater, J. G., *Geophys. J. R. Astron. Soc.*, 1971, **25**, 437–528.
2. Sclater, J. G. and Fisher, R. L., *Soc. Am. Bull.*, 1974, **85**, 683–702.
3. Schlich, R., in *The Basins and Margins, The Indian Ocean* (eds

Nairn, A. E. and Stehli, F. G.), Plenum, New York, 1982, vol. 6, pp. 51–147.
4. Royer, J. Y. and Schlich, R., *J. Geophys. Res.*, 1988, **93**, 13524–13550.
5. Patriat, P. J. and Segoulin, J., *Tectonophysics*, 1988, **155**, 211–234.
6. Royer, J. Y., Sclater, J. G. and Sandwell, D. T., *Proc. Indian Acad. Sci. (Earth Planet. Sci.)*, 1989, **98**, 7–24.
7. Munschy, M. and Schlich, R., *Mar. Geophys. Res.*, 1989, **11**, 1–14.
8. Bergman, E. A. and Solomon, S. C., *Phys. Earth Planet Inter.*, 1985, **40**, 1–23.
9. Petroy, D. E. and Weins, D. A., *J. Geophys. Res.*, **94**, 12301–12326.
10. Stein, C. A., Cloatingh, S. A. P. L. and Wortel, M. J. R., Proc. Ocean Drilling Proj. Sci. Results, Leg 116, 1989b.
11. Stein, C. A. and Weissel, J. K., *Tectonophysics*, 1990, **176**, 315–332.
12. Eittreim, S. L. and Ewing, *J. Geophys. Res.*, 1972, **77**, 6413–6421.
13. Weissel, J. K., Anderson, R. N. and Geller, C. A., *Nature*, 1980, **287**, 284–291.
14. Neprochnov, Y. P., Levchenko, O. V. and Sedov, V. V., *Tectonophysics*, 1988, **156**, 89–106.
15. Bull, J. M., *Tectonophysics*, 1990, **184**, 213–228.
16. Bull, J, M. and Scrutton, R. A., *Nature*, 1990, **344**, 855–858.
17. Bull, J. M. and Scrutton, R. A., *J. Geol. Soc. London*, 1992, **144**, 955–966.
18. Geller, C. A., Weissel, J. K. and Anderson, R. N., *Tectonics*, 1983, **9**, 409–422.
19. Kahle, H. G., Naini, B. R., Talwani, M. and Eldholm, O., *J. Geophys. Res.*, 1981, **86**, 3807–3814.
20. Gordon, R. G. and DeMets, C., *Tectonics*, 1990, **9**, 409–422.
21. Kamesh Raju, K. A. and Ramprasad, T., *Earth Planet. Sci. Lett.*, 1989, **95**, 395–402.
22. Neprochnov, Yu. P., Levchenko, O. V. and Merklin, L. R., *Geotectonics*, 1985, **1**, 15–23.
23. Levchenko, O. V., Evsjukov, Y. D., Subrahmanyam, C., Mital, G. S. and Drolia, R. K., *Marine Geol.*, 1993, **115**, 165–171
24. John, L., LaBreque, Dennis, V. Kent and Steven C. Cande, Lamont-Doherty Geological Observatory Contribution No. 2399, 1977.
25. Rajendran, S., Ph D thesis, Andhra University, 1995.
26. Raval, U., Proceedings of the 29th Annual Convention, Indian Geophysical Union, 1993, pp. 104–114.
27. Talwani, M. and Eldholm, O., *Geol. Soc. Am. Bull.*, 1972, **83**, 3575– 3606.
28. Talwani, M. and Eldholm, O., *Nature*, 1973, **241**, 325–330.
29. Scrutton, R. A. and DuPlessis, A., *Nature*, 1973, **242**, 180–182.
30. Scrutton, R. A., *Geophys. J. R. Astron. Soc.*, 1976, **44**, 601– 623.
31. Talwani, M., *An. Acad. Brasil Cienc.*, 1976, **48**, 337–352.
32. Rabinowitz, and LaBrecque, *Earth Planet. Sci. Lett.*, 1977, **35**, 145–150.

ACKNOWLEDGEMENTS. We thank Late Dr H. N. Siddiquie, Former Director of National Institute of Oceanography, Goa for permitting to participate in the Central Indian Ocean cruise and for providing magnetic data. Our sincere thanks are due to Dr C. G. Nambiar, Department of Marine Geology and Geophysics, Cochin University for his valuable suggestions.

Received 2 June 1999; revised accepted 7 March 2000

Ujjain clay as low-cost sealant and liner for artificial ponding and bentonite alternative

S. K. Billore*,†, N. Singh*, J. K. Sharma*, R. Krishnamurthi, Taisuke Kobayashi# and Reiko Yagi‡**

*Institute of Environment Management and Plant Sciences, Vikram University, Ujjain 456 010, India
**School of Studies in Geology, Vikram University, Ujjain 456 010, India
#Department of Earth Sciences, Chiba University, 1-33 Yayoi-cho, Inage-ku, Chiba 263, Japan
‡Natural History Museum & Institute, Chiba 955-2, Aoba-cho, Chiba 260, Japan

Synthetic and natural clay (bentonite) liners are commercially used to protect leakage from a variety of earthy ponding and containments in order to conserve water and for the wastewater not to contaminate the groundwater. The present study evaluates the sealant property of the local clay hitherto used intensively in the manufacture of earthenwares, bricks, smearing materials and sealant in roof cracks. Extensive deposits of fluvial sediments occur along the bank of River Kshipra in and around Ujjain situated on Malwa plateau in Madhya Pradesh. Field-collected clay samples were analysed by X-ray diffraction and ethylene glycol treatment (EGT), and compared with standard bentonite procured from Gujarat Mineral Development Corporation. The X-ray diffraction profile analysis with basal reflection (001) at 14° to 15° clearly confirmed the identification of smectite group of the clay under study. The EGT substantiated the presence of smectite in the Ujjain clay as well as in the standard bentonite, which is diagnostic to the swelling property of the clay. The overall study thus characterizes the potentiality of Ujjain clay as a mineral-based hydraulic barrier material and a component of natural liner in surface-water impoundments and lagoons.

WATER and wastewater being resources in tropical India, have been subjected to loss through downward and sideward seeping from stationary and mobile waterbodies, such as small-scale freshwater/industrial ponds, lagoons, lakes, storage dams and reservoirs, irrigation canals, constructed wetlands[1], sewage effluent irrigation, landfill sites, etc. To control this loss, synthetic polymers such as PVC, plastic, heavy and low density polyethylene (HDPE and LDPE)[2], fibertex, geotextile and naturally occurring commercial bentonite clay are in vogue as sheet piling, but are expensive items as liners. Swelling to several times its original volume when wet, the bentonite layer is able to seal potential leaks in the artificial ponds and acts as an excellent hydraulic barrier[3].

The yellow clay deposits occur in the form of fluvial sediments with ridges and linear bars along the bank of

†For correspondence. (e-mail: billore@bom4.vsnl.net.in)